

# CHARACTERISATION OF Mo(VI) OXO-SPECIES ON THE SURFACE OF THE RATIONALLY DESIGNED MoO<sub>3</sub>/Al<sub>2</sub>O<sub>3</sub> and MoO<sub>3</sub>/SiO<sub>2</sub> MODEL SYSTEMS

Yu.V. Plyuto, L.F. Sharanda, D.B. Nasedkin, I.V. Babich

Chuiiko Institute of Surface Chemistry, National Academy of Sciences of Ukraine,  
17 Oleh Mudrak Str., 03164 Kyiv, Ukraine, e-mail: yuri.plyuto@isc.gov.ua

*Model well-defined MoO<sub>3</sub>/Al<sub>2</sub>O<sub>3</sub> and MoO<sub>3</sub>/SiO<sub>2</sub> systems were rationally designed by anchoring of MoOCl<sub>4</sub> on the supports surface of fumed Al<sub>2</sub>O<sub>3</sub> and SiO<sub>2</sub> nanoparticles. The subsequent hydrolysis of the anchored groups by water vapours followed by thermal treatment resulted in the formation of Mo(VI) oxo-species on the supports surface. By application of the anchoring – hydrolysis cycles the model MoO<sub>3</sub>/Al<sub>2</sub>O<sub>3</sub> systems with the molybdena loading of 1.10, 1.92 and 2.34 Mo/nm<sup>2</sup> were synthesised. The synthesised MoO<sub>3</sub>/SiO<sub>2</sub> systems had a molybdena loading of 0.82, 1.05 and 1.21 Mo/nm<sup>2</sup>. X-ray diffraction patterns characteristic for MoO<sub>3</sub> crystallites were not observed in the synthesised MoO<sub>3</sub>/Al<sub>2</sub>O<sub>3</sub> and MoO<sub>3</sub>/SiO<sub>2</sub> systems up to the highest achieved molybdena loading of 2.34 and 1.21 Mo/nm<sup>2</sup> respectively. This confirms that the used preparation route resulted in the formation of highly dispersed Mo(VI) oxo-species on the surface of both Al<sub>2</sub>O<sub>3</sub> and SiO<sub>2</sub> supports. The degree of aggregation of Mo(VI) oxo-species depends on the nature of the support surface and molybdena loading. Increase of the molybdena loading on the surface of both Al<sub>2</sub>O<sub>3</sub> and SiO<sub>2</sub> supports results in an increase of the degree of aggregation of Mo(VI) oxo-species. On Al<sub>2</sub>O<sub>3</sub> support, at a molybdena loading which corresponds to the population of surface hydroxyl groups, monomeric Mo(VI) oxo-species appear to be predominant. At higher molybdena loading, the formation of polymeric Mo(VI) oxo-species was detected. On SiO<sub>2</sub> support, at a molybdena loading which corresponds or exceeds the population of surface hydroxyl groups, simultaneous presence of monomeric and polymeric Mo(VI) oxo-species was observed.*

**Keywords:** Alumina, silica, supports surface chemistry, molybdena, surface oxo-species, UV-Vis spectroscopy.

## INTRODUCTION

The in-depth study of the structure of surface Mo(VI) oxo-species is the subject of standing interest using modern experimental techniques [1–5] and theoretical methods [6–9]. A number of studies aiming at the development of new approaches to the synthesis of alumina and silica supported molybdenum systems were undertaken. Anchoring of inorganic and organometallic molybdenum compounds, namely MoCl<sub>5</sub> [10–12], MoOCl<sub>4</sub> [13], MoO<sub>2</sub>Cl<sub>2</sub> [14, 15], MoO<sub>2</sub>(acac)<sub>2</sub> [16] and Mo( $\pi$ -C<sub>3</sub>H<sub>5</sub>)<sub>4</sub> [17] on the support surface was realised.

Catalytic activity of alumina and silica supported molybdenum oxide systems in the reactions of selective oxidation, hydrodesulfurisation, oxidative coupling and metathesis are widely known [18–21]. Commercial importance of these processes stimulates the basic studies aiming at modelling of the active phase - support interaction at a molecular level which is considered as one of the most significant factors influencing the dispersion of the supported Mo(VI) oxo-species and consequently the structure of the catalytically active sites.

Anchoring of inorganic and organometallic molybdenum compounds is considered to be the best alternative to the conventional impregnation technique for the synthesis of model supported molybdenum systems [22] and their characterisation [23]. Firstly, anchoring is free of

disadvantages from which impregnation suffers. If a solvent is used, its removal occurs when molybdenum inorganic or organometallic compound is chemically attached to the support surface and therefore aggregation of the Mo(VI) oxo-species is minimised. As a result, the problems of samples inhomogeneity are overcome to a large extent. Secondly, anchoring creates conditions under which a maximum spreading of Mo(VI) oxo-species on the support surface has to be expected. Their concentration appears to be equivalent to the population of surface hydroxyl groups of the initial support which are considered to be responsible for the formation of the dispersed Mo(VI) oxo-species.

Upon anchoring of molybdenum inorganic or organometallic compound to the support of well defined structure one may expect the formation of uniform surface species. Highly dispersed fumed alumina and silica supports which possess a micropore free texture fit this requirement and are suitable for studies aiming at modelling of the molybdena phase - support interaction.

The aims of this work are to design model  $\text{MoO}_3/\text{Al}_2\text{O}_3$  and  $\text{MoO}_3/\text{SiO}_2$  systems and to investigate how the degree of Mo(VI) oxo-species aggregation depends on the nature of alumina and silica supports.

In this study, model  $\text{MoO}_3/\text{Al}_2\text{O}_3$  and  $\text{MoO}_3/\text{SiO}_2$  systems were synthesised by anchoring of  $\text{MoOCl}_4$  followed by hydrolysis and subsequent thermal treatment that resulted in the formation of Mo(VI) oxo-species. The synthesised model systems were characterised by a diffuse reflectance UV-Vis spectroscopy.

It is reasonable to expect that the preparation route based on anchoring of molybdenum inorganic or organometallic compound on the surface of fumed alumina and silica has to result in spreading of Mo(VI) oxo-species which is governed essentially by their specific interaction with the supports.

## EXPERIMENTAL

$\text{MoO}_3/\text{Al}_2\text{O}_3$  and  $\text{MoO}_3/\text{SiO}_2$  samples were synthesised by using a highly pure, well-defined alumina (Aluminium Oxide C, specific surface of  $100 \text{ m}^2/\text{g}$ , average primary particle size of 13 nm) and silica (AEROSIL 200, specific surface of  $200 \text{ m}^2/\text{g}$ , specific surface of 12 nm) supports. Supports were pelleted by pressing, crushed and sieved. The fraction of 0.25–0.50 mm was used.

About 1 g of the support dehydrated at  $200^\circ\text{C}$  was treated with 30 ml of 0.01 M solution of  $\text{MoOCl}_4$  (Aldrich) in dichloromethane (Baker) which was dried with molecular sieves. Treatment was carried out at  $40^\circ\text{C}$  for 1 h under a flow of dry nitrogen. In order to achieve the maximum molybdena loading the supernatant was replaced by a fresh  $\text{MoOCl}_4$  solution twice.

The synthesised samples were thoroughly washed with dichloromethane which was removed by evacuation. For the removal of chlorine from the synthesised samples, they were left overnight for hydrolysis with water vapour ( $p/p_s=0.75$ ) at room temperature followed by dehydration at  $200^\circ\text{C}$  for 2 h.

In order to prepare samples with an increased molybdena loading, the above mentioned anchoring-hydrolysis cycle was repeated.

The as-prepared samples were calcined in air at  $500^\circ\text{C}$  for 4 h. The total molybdenum content was determined by AAS after treatment of the calcined samples with a hot 2 M aqueous potassium hydroxide.

X-ray powder diffractograms in the  $2\theta$  region of  $5\text{--}60^\circ$  were measured on a Philips PW 1840 diffractometer using  $\text{Cu K}\alpha$  radiation.

UV-Vis spectra were registered against blanks of barium sulfate in the region 200 - 900 nm using a Cary 3 UV-Vis spectrophotometer with a diffuse reflectance accessory. The results were expressed in the form of the Kubelka-Munk function.

## RESULTS AND DISCUSSION

The synthesis of MoO<sub>3</sub>/Al<sub>2</sub>O<sub>3</sub> and MoO<sub>3</sub>/SiO<sub>2</sub> systems was carried out by anchoring MoOCl<sub>4</sub> on the hydroxylated surface of alumina and silica supports. Anchoring occurred via chemical reaction of the MoOCl<sub>4</sub> molecules with surface hydroxyl groups [13, 24, 25]



The hydrolysis of (---O)<sub>n</sub>MoOCl<sub>4-n</sub> groups enabled to repeat MoOCl<sub>4</sub> anchoring. Subsequent thermal treatment resulted in the formation of Mo(VI) oxo-species on the support surface.

According to AAS analysis, the molybdena loading in the synthesised alumina and silica samples was found to be dependent on the type of the support as well as on the number of anchoring-hydrolysis cycles.

Fig. 1 illustrates how number of anchoring-hydrolysis cycles influences the molybdena loading in the synthesised silica and alumina supported samples. It is clearly seen that in both cases repetition results in an increase of molybdena loading although this increase is smaller in each next cycle. This means that the molybdena loading approaches saturation.

Application of the described preparation route resulted in the synthesis of alumina samples with a molybdena loading which corresponds to 1.10, 1.92 and 2.34 Mo/nm<sup>2</sup>, denoted hereafter as MoO<sub>3</sub>(1.10)/Al<sub>2</sub>O<sub>3</sub>, MoO<sub>3</sub>(1.92)/Al<sub>2</sub>O<sub>3</sub> and MoO<sub>3</sub>(2.34)/Al<sub>2</sub>O<sub>3</sub>, respectively. The synthesised silica samples with a molybdena loading of 0.82, 1.05 and 1.21 Mo/nm<sup>2</sup> are denoted as MoO<sub>3</sub>(0.82)/SiO<sub>2</sub>, MoO<sub>3</sub>(1.05)/SiO<sub>2</sub> and MoO<sub>3</sub>(1.21)/SiO<sub>2</sub>, correspondingly.

Repetition of the anchoring-hydrolysis cycles enables to reach higher molybdena loading on the alumina support in comparison with that on silica (Fig. 1). This is in agreement with higher population of hydroxyl groups on alumina surface which are responsible for anchoring of MoOCl<sub>4</sub> (see eq. 1). After dehydration at 500 °C, the population of hydroxyl groups on alumina support was reported to be at least two times higher than that on silica [26].

A possibility of repetition of the anchoring-hydrolysis cycles reflects regeneration of surface hydroxyl groups which are consumed when MoOCl<sub>4</sub> anchoring occurs (see eq. 1). This means at least partial hydrolysis of the anchored (---O)<sub>n</sub>MoOCl<sub>4-n</sub> groups accompanied by the reappearance of surface hydroxyl groups and the formation of molybdenum (VI) oxo-species.

It is clearly seen that each subsequent anchoring-hydrolysis cycle results in an increase of molybdena loading although this increase appears to be smaller in each next cycle. As surface hydroxyl groups are responsible for MoOCl<sub>4</sub> anchoring (eq. 1), this is explained by a decrease of their total population upon repetition of anchoring-hydrolysis cycles. The observed progressive decrease of population of surface hydroxyl groups means that the number of Mo(VI) oxo-species which are covalently bound to the support surface increases.

X-ray diffraction patterns of the synthesised MoO<sub>3</sub>/Al<sub>2</sub>O<sub>3</sub> and MoO<sub>3</sub>/SiO<sub>2</sub> systems (Fig. 2) revealed diffraction maxima similar to those of Aluminium Oxide C (γ-Al<sub>2</sub>O<sub>3</sub>) and a very broad pattern around 10–40° (2θ) typical for AEROSIL 200 (amorphous SiO<sub>2</sub>). The diffraction patterns characteristic for MoO<sub>3</sub> crystallites were not observed. XRD patterns of the synthesised MoO<sub>3</sub>(2.34)/Al<sub>2</sub>O<sub>3</sub> and MoO<sub>3</sub>(1.21)/SiO<sub>2</sub> systems with the highest achieved molybdena loading of 2.34 and 1.21 Mo/nm<sup>2</sup> are presented in Fig. 2.

This confirms that the used preparation route resulted in the formation of highly dispersed Mo(VI) oxo-species on the surface of both supports. The main reason is the correspondence of the molybdena loading to the population of surface hydroxyl groups [27] which is achieved by the anchoring of MoOCl<sub>4</sub> to the support surface. Therefore, one has to come to the conclusion that on both supports the highly dispersed Mo(VI) oxo-species exist being interacted with the support surface.

Diffuse reflectance UV-Vis spectra of the synthesised samples are shown in Fig. 3 and

Fig. 4. In both cases the strong absorption is observed in the region of 200–400 nm because of the ligand to metal  $O^{2-} \rightarrow Mo^{6+}$  charge transfer [28, 29]. No absorbance above 800 nm which might be attributed to the reduced Mo(VI) oxo-species [10–12] is seen. For the synthesised samples a better resolution of the absorption bands is observed in comparison with  $MoO_3/Al_2O_3$  and  $MoO_3/SiO_2$  systems prepared by impregnation [30–32]. The presence of well resolved absorption bands indicates the uniform structure of Mo(VI) oxo-species on the surface of  $Al_2O_3$  and  $SiO_2$  supports.

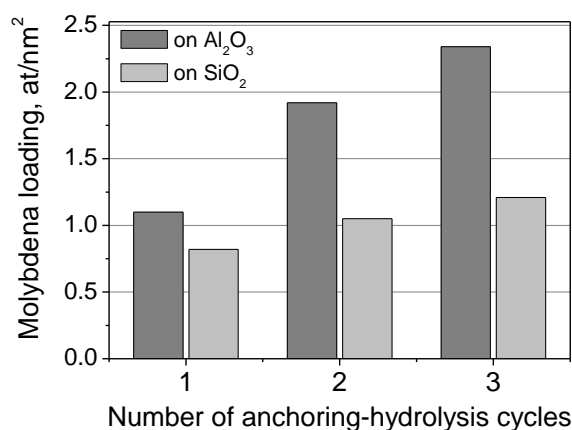


**Fig. 1.** Molybdena loading in the synthesized  $MoO_3/Al_2O_3$  and  $MoO_3/SiO_2$  systems

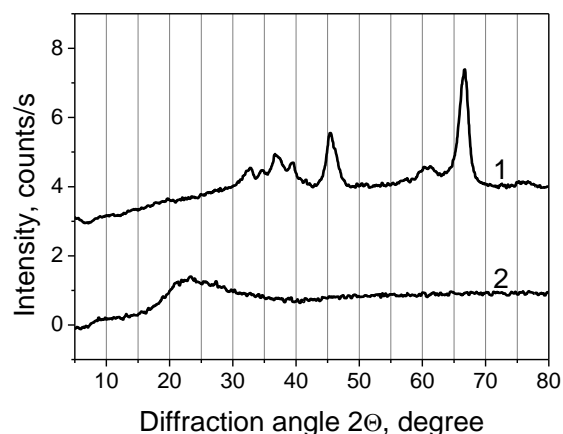


**Fig. 2.** XRD patterns of the synthesized  $MoO_3(2.34)/Al_2O_3$  – 1 and  $MoO_3(1.21)/SiO_2$  – 2 systems

For  $MoO_3/Al_2O_3$  and  $MoO_3/SiO_2$  systems different coordination environments of  $Mo^{6+}$  ions in surface Mo(VI) oxo-species, namely  $Mo^{6+}$  in tetrahedral ( $T_d$ ) and octahedral ( $O_h$ ) coordination may be distinguished with UV-Vis spectroscopy [30, 31, 33, 34]. The band at 230 nm is common for both  $Mo^{6+}$  ( $T_d$ ) and  $Mo^{6+}$  ( $O_h$ ) ions whereas absorption in 280–295 nm spectral region is connected only with  $Mo^{6+}$  ( $O_h$ ) ions.

From Fig. 3 and Fig. 4 one may see a distinct difference of the UV-Vis spectra of Mo(VI) oxo-species on the surface of  $Al_2O_3$  and  $SiO_2$  supports.

In the case of  $MoO_3(1.10)/Al_2O_3$  sample (Fig. 3.1), a strong absorption band at 220 nm is observed. The increase of the molybdena loading from 1.10 to 1.92  $Mo/nm^2$  results not only in an increase of the intensity of the band at 220 nm but also in the appearance of the intensive band at 270 nm (Fig. 3.2) which is seen as a broad shoulder in the spectrum of the sample with low molybdena loading (Fig. 3.1). Further increase of the molybdena loading to 2.34  $Mo/nm^2$  results in simultaneous growth of intensity of the both bands (Fig. 3.3). Therefore we may conclude that  $Mo^{6+}$  in surface Mo(VI) oxo-species at a molybdena loading which does not exceed 1.10  $Mo/nm^2$  is preferably tetrahedrally coordinated. At higher molybdena loading, Mo(VI) oxo-species in which  $Mo^{6+}$  possesses both tetrahedral and octahedral coordination are present on the  $Al_2O_3$  surface.

In the diffuse reflectance UV-Vis spectrum of all  $MoO_3/SiO_2$  samples (Fig. 4) one can observe a strong absorption around 280–295 nm and at 220 nm. Simultaneous increase of the intensity of these bands with the rise of molybdena loading leads to the conclusion that  $Mo^{6+}$  in surface Mo(VI) oxo-species on the silica surface have preferably octahedral coordination. Of course, the presence of the tetrahedrally coordinated  $Mo^{6+}$  ions in surface Mo(VI) oxo-species on  $SiO_2$  support can not be precluded since the band at 220 nm has to be attributed to both  $Mo^{6+}$  ( $T_d$ ) and  $Mo^{6+}$  ( $O_h$ ).

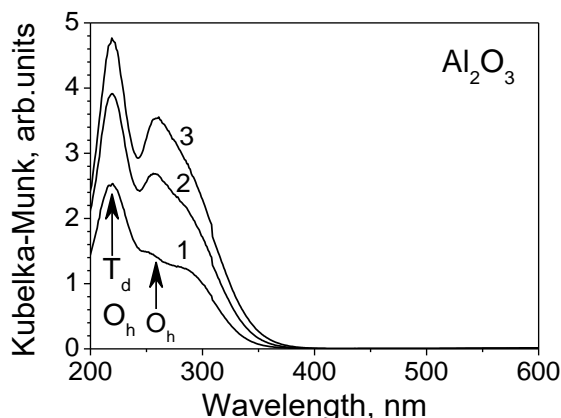


**Fig. 3.** Diffuse reflectance UV-Vis spectra of the synthesised  $\text{MoO}_3(1.10)/\text{Al}_2\text{O}_3$  – 1,  $\text{MoO}_3(1.92)/\text{Al}_2\text{O}_3$  – 2 and  $\text{MoO}_3(2.34)/\text{Al}_2\text{O}_3$  – 3 systems

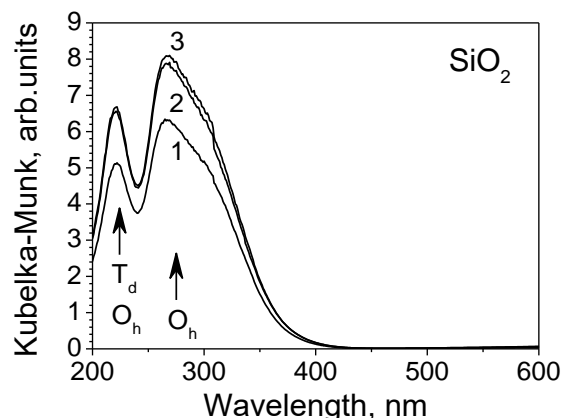


**Fig. 4.** Diffuse reflectance UV-Vis spectra of the synthesised  $\text{MoO}_3(0.82)/\text{SiO}_2$  – 1,  $\text{MoO}_3(1.05)/\text{SiO}_2$  – 2 and  $\text{MoO}_3(1.21)/\text{SiO}_2$  – 3 systems

Naturally, surface Mo(VI) oxo-species differ in the degree of aggregation and a way in which they interact with the support. It is reasonable to imagine two principal types of Mo(VI) oxo-species, namely monomeric isolated Mo(VI) oxo-species and polymeric Mo(VI) oxo-species which can form a monolayer like phase. These structures are presented in a simplified form in Fig. 5 and Fig. 6.

The diffuse reflectance UV-Vis spectra of  $\text{MoO}_3/\text{Al}_2\text{O}_3$  and  $\text{MoO}_3/\text{SiO}_2$  systems confirm a difference in coordination environment of  $\text{Mo}^{6+}$  ions in surface Mo(VI) oxo-species and enable to clarify some details of the degree of their aggregation on  $\text{Al}_2\text{O}_3$  and  $\text{SiO}_2$  supports. In order to do this, one has to take into account that in monomeric Mo(VI) oxo-species  $\text{Mo}^{6+}$  ion has essentially tetrahedral coordination while aggregation results in an increase of its coordination environment to octahedral.

In the  $\text{MoO}_3(1.10)/\text{Al}_2\text{O}_3$  sample, essentially monomeric Mo(VI) oxo-species are present as tetrahedrally coordinated  $\text{Mo}^{6+}$  ions are observed (Fig. 3.1). It is clear that only in monomeric Mo(VI) oxo-species which are stabilised on the surface of  $\text{Al}_2\text{O}_3$  support (Fig. 5) tetrahedral coordination can be realised.

In  $\text{MoO}_3(1.92)/\text{Al}_2\text{O}_3$  and  $\text{MoO}_3(2.34)/\text{Al}_2\text{O}_3$  samples, aggregated Mo(VI) oxo-species are present (Fig. 6) since  $\text{Mo}^{6+}$  ions possessing octahedral coordination are observed in UV-Vis spectra (Fig. 3.2 and Fig. 3.3). The presence of the monomeric Mo(VI) oxo-species can not be precluded because of limitations of UV-Vis spectroscopy in detection of the tetrahedrally coordinated  $\text{Mo}^{6+}$  when octahedrally coordinated  $\text{Mo}^{6+}$  are present.

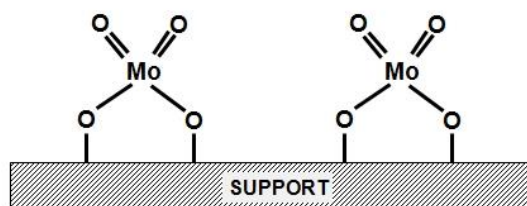


**Fig. 5.** Monomeric Mo(VI) oxo-species on the support surface

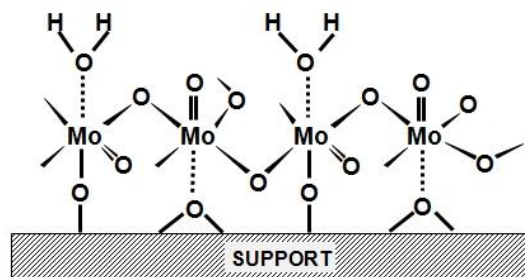


**Fig. 6.** Polymeric Mo(VI) oxo-species on the support surface

In MoO<sub>3</sub>(0.82)/SiO<sub>2</sub>, MoO<sub>3</sub>(1.05)/SiO<sub>2</sub> and MoO<sub>3</sub>(1.21)/SiO<sub>2</sub> samples mainly aggregated Mo(VI) oxo-species are present (Fig. 6) since octahedrally coordinated Mo<sup>6+</sup> ions are observed in UV-Vis spectra (Fig. 4). As the tetrahedrally coordinated Mo<sup>6+</sup> ions can not be discriminated by UV-Vis from octahedrally coordinated when the latter are present, the presence of monomeric Mo(VI) oxo-species can not be ruled out in these samples.

## CONCLUSIONS

The model well-defined MoO<sub>3</sub>/Al<sub>2</sub>O<sub>3</sub> and MoO<sub>3</sub>/SiO<sub>2</sub> systems may be rationally designed by anchoring of MoOCl<sub>4</sub> on the supports surface of fumed Al<sub>2</sub>O<sub>3</sub> and SiO<sub>2</sub> nanoparticles. The subsequent hydrolysis by water vapours and followed by thermal treatment resulted in the formation of Mo(VI) oxo-species on the supports surface. By application of the anchoring – hydrolysis cycles model MoO<sub>3</sub>/Al<sub>2</sub>O<sub>3</sub> systems with the molybdena loading of 1.10, 1.92 and 2.34 Mo/nm<sup>2</sup> were synthesised. The synthesised MoO<sub>3</sub>/SiO<sub>2</sub> systems had a molybdena loading of 0.82, 1.05 and 1.21 Mo/nm<sup>2</sup>.

X-ray diffraction patterns characteristic for MoO<sub>3</sub> crystallites were not observed in the synthesised MoO<sub>3</sub>/Al<sub>2</sub>O<sub>3</sub> and MoO<sub>3</sub>/SiO<sub>2</sub> systems up to the highest achieved molybdena loading of 2.34 and 1.21 Mo/nm<sup>2</sup> respectively. This confirms that the used preparation route resulted in the formation of highly dispersed Mo(VI) oxo-species on the surface of both Al<sub>2</sub>O<sub>3</sub> and SiO<sub>2</sub> supports.

The degree of aggregation of Mo(VI) oxo-species were found to be dependent on the nature of the support surface and molybdena loading. Increase of the molybdena loading on the surface of both Al<sub>2</sub>O<sub>3</sub> and SiO<sub>2</sub> supports results in an increase of the degree of aggregation of Mo(VI) oxo-species.

On Al<sub>2</sub>O<sub>3</sub> support, at a molybdena loading which corresponds to the population of surface hydroxyl groups, monomeric Mo(VI) oxo-species appear to be predominant. At higher molybdena loading, the formation of polymeric Mo(VI) oxo-species was detected. On SiO<sub>2</sub> support, at a molybdena loading which corresponds or exceeds the population of surface hydroxyl groups, simultaneous presence of monomeric and polymeric Mo(VI) oxo-species was observed.

This work was financially supported by the European Union under Supplementary Agreement N<sup>o</sup> ERB CIPD CT 940510 to Contract N<sup>o</sup> ERB J0U2 CT 930409.

## REFERENCES

1. Li L., Scott S. L. X-ray Absorption Spectroscopy Investigation into the Origins of Heterogeneity in Silica-Supported Dioxomonomolybdates. *J. Phys. Chem. C*. 2021. **125**(42): 23115.
2. Savinelli R. O., Scott, S. L. Wavelet transform EXAFS analysis of mono- and dimolybdate model compounds and a Mo/HZSM-5 dehydroaromatization catalyst. *Phys. Chem. Chem. Phys.* 2010. **12**(21): 5660.
3. Yamamoto K., Chan K. W., Mougél V., Nagae H., Tsurugi H., Safonova O. V., Mashima K., Copéret C. Silica-supported isolated molybdenum di-oxo species: formation and activation with organosilicon agent for olefin metathesis. *Chem. Commun.* 2018. **54**(32): 3989.
4. Berkson Z. J., Bernhardt M., Schlapansky S. L., Benedikter M. J., Buchmeiser M. R., Price G. A., Sunley G. J., Copéret Ch. Olefin-Surface Interactions: A Key Activity Parameter in Silica-Supported Olefin Metathesis Catalysts. *JACS Au*. 2022. **2**: 777.
5. Berkson Z. J., Zhu R., Ehinger Ch., Lätsch L., Schmid S. P., Nater D., Pollitt S., Safonova O. V., Björgvinsdóttir S., Barnes A. B., Román-Leshkov Y., Price G. A., Sunley G. J., Copéret Ch. Active Site Descriptors from <sup>95</sup>Mo NMR Signatures of Silica-Supported Mo-Based Olefin Metathesis Catalysts. *J. Am. Chem. Soc.* 2023. **145**: 12651.

6. Guo C.S., Hermann K., Havecker M., Thielemann J.P., Kube P., Gregoriades L.J., Trunschke A., Sauer J., Schlögl R. Structural Analysis of Silica-Supported Molybdena Based on X-ray Spectroscopy: Quantum Theory and Experiment. *J. Phys. Chem. C*. 2011. **115**(31): 15449.
7. Handzlik J., Kurlito K., Gierada M. Computational Insights into Active Site Formation during Alkene Metathesis over a  $\text{MoO}_x/\text{SiO}_2$  Catalyst: The Role of Surface Silanols. *ACS Catal.* 2021. **11**: 13575.
8. Kurlito K., Tielens F., Handzlik J. Isolated Molybdenum(VI) and Tungsten(VI) Oxide Species on Partly Dehydroxylated Silica: A Computational Perspective. *J. Phys. Chem. C*. 2020. **124**(5): 3002.
9. Nasiedkin D.B., Nazarchuk M.O., Grebenyuk A.G., Sharanda L.F., Plyuto Yu.V. Quantum chemical simulation of  $\text{MoO}_3$  dispergation on hydroxylated  $\text{SiO}_2$  surface. *Surface*. 2021 **13**(28): 75.
10. Louis C., Che. M. EPR and diffuse reflectance studies of the physico-chemical phenomena occurring during the preparation of  $\text{Mo}/\text{SiO}_2$  catalysts by the grafting method. *J. Catal.* 1992. **135**: 156.
11. Louis C., Che M., Anpo M. Characterization and modeling of the Mo species in grafted  $\text{Mo}/\text{SiO}_2$  catalysts after redox thermal treatments. *J. Catal.* 1993. **141**: 453.
12. Fricke R., Hanke W., Ohlmann G. Studies on catalytically active surface compounds: IV. Preparation of  $\text{Mo}/\text{SiO}_2$  catalysts from  $\text{MoCl}_5$  studied by ESR and UV-vis spectroscopy. *J. Catal.* 1983. **79**: 1.
13. Maksimowski P., Skupinski W. Catalytic activity of supported tungsten and molybdenum complexes in olefin metathesis. *J. Mol Catal.* 1991. **65**: 187.
14. Jason K., Jun-Young J., In-Gyu Ch., Yeong-Cheol K.. Search for adsorption geometry of precursor on surface using genetic algorithm:  $\text{MoO}_2\text{Cl}_2$  on  $\text{SiO}_2$  surface. *J. Korean Ceram. Soc.* 2020. **57**: 669.
15. Kim H.-K., Lee N.-Y., Kim Y.-Ch. Evaluation of vapor pressure of  $\text{MoO}_2\text{Cl}_2$  and its initial chemical reaction on a  $\text{SiO}_2$  surface by ab initio thermodynamics. *Curr. Appl. Phys.* 2024. **61**: 115.
16. Handzlik J., Ogonowski J., Stoch J., Mikolajczyk M. Comparison of metathesis activity of catalysts prepared by anchoring of  $\text{MoO}_2(\text{acac})_2$  on various supports. *Catal. Lett.* 2005. **101**(1–2): 65.
17. Iwasawa Y., Ogasawara S. Spectroscopic study on the surface structure and environment of fixed Mo catalysts prepared by use of  $\text{Mo}(\pi\text{-C}_3\text{H}_5)_4$ . *J. Chem. Soc., Faraday Trans.* 1979. **1**: 1465.
18. Haber J. Molybdenum Compounds in Heterogeneous Catalysis. *Stud. Inorg. Chem.* 1994. **19**: 477.
19. Topsøe H., Clausen B.S., Massoth F.E. Hydrotreating Catalysis. In: *Catalysis. Catalysis-Science and Technology* (Berlin: Springer, 1996).
20. Lwin S., Wachs I. E. Olefin Metathesis by Supported Metal Oxide Catalysts. *ACS Catalysis*. 2014. **4**(8): 2505.
21. Fierro J. L. G., Mol J. C. Metathesis of Olefins on Metal Oxides. In: *Metal Oxides: Chemistry and Applications* (Boca Raton, FL: CRC Press, 2006).
22. Iwasawa Y. Chemical Design Surfaces for Active Solid Catalysts. In: *Advances in Catalysis* (Orlando, FL: Academic Press. Inc., 1987).
23. Massoth E. F. Characterization of Molybdena Catalysts. *Adv. Catal.* 1978. **27**: 265.
24. Patent EP 2 985 077 A1. Mostafa T., Philipse H. J. F., Garro, A., Norsic S., Szeto K., Rouge P. Supported molybdenum or tungsten complexes, its preparation and use in olefin metathesis.

25. Gun'ko V. M., Chuiko A. A. Chemical Reactions at Fumed Silica Surfaces. In *Colloidal Silica: Fundamentals and Applications* (Boca Raton, FL: Taylor & Francis, 2005).
26. Schreiber L. B., Vaughan R. W. A nuclear magnetic resonance investigation of high surface area silica-aluminas. *J. Catal.* 1975 **40**: 226.
27. Roark R. D., Kohler S. D., Ekerdt J. G. Role of silanol groups in dispersing Mo(VI) on silica. *Catal. Lett.* 1992. **16**: 71.
28. Fournier M., Louis C., Che M., Chaquin P., Masure D. Polyoxometallates as models for oxide catalysts : Part I. An UV-visible reflectance study of polyoxomolybdates: Influence of polyhedra arrangement on the electronic transitions and comparison with supported molybdenum catalysts. *J. Catal.* 1989. **119**: 400.
29. Masure D., Chaquin P., Louis C., Che M., Fournier M. Polyoxometallates as models for oxide catalysts : Part II. Theoretical semi-empirical approach to the influence of the inner and outer Mo coordination spheres on the electronic levels of polyoxomolybdates. *J. Catal.* 1989. **119**: 415.
30. Williams C. C., Ekerdt J. G., Jehng J.-M., Hardcastle F. D., Turek A. M., Wachs I. E. A Raman and ultraviolet diffuse reflectance spectroscopic investigation of silica-supported molybdenum oxide. *J. Phys. Chem.* 1991. **95**: 8781.
31. Williams C. C., Ekerdt J. G., Jehng J.-M., Hardcastle F. D., Wachs I. E. A Raman and ultraviolet diffuse reflectance spectroscopic investigation of alumina-supported molybdenum oxide. *J. Phys. Chem.* 1991. **95**: 8791.
32. Liu T. C., Forissier M., Coudurier G., Vedrine J. C. Properties of molybdate species supported on silica. *J. Chem. Soc., Faraday Trans.* 1989. **1**: 1607.
33. Caceres C. V., Fierro J. L. G., Lopez A. A., Blanco M. N., Thomas H. J. Preparation and characterization of equilibrium adsorption-prepared molybdena-alumina catalysts. *J. Catal.* 1985. **95**: 501.
34. Morey, M. S.; Bryan, J. D.; Schwarz, S.; Stucky, G. D. Pore Surface Functionalization of MCM-48 Mesoporous Silica with Tungsten and Molybdenum Metal Centers: Perspectives on Catalytic Peroxide Activation. *Chem. Mat.* 2000. **12**(11): 3435.

PACS: 81.07.-b; 61.05.cp; 29.30.Dn

DOI: 10.15407/Surface.2024.16.164

## ДОСЛІДЖЕННЯ Mo(VI) ОКСО-СТРУКТУР НА ПОВЕРХНІ ЦІЛЕСПРЯМОВАНО СТВОРЕНИХ МОДЕЛЬНИХ СИСТЕМ MoO<sub>3</sub>/Al<sub>2</sub>O<sub>3</sub> ТА MoO<sub>3</sub>/SiO<sub>2</sub>

Ю.В. Плюто, Л.Ф. Шаранда, Д.Б. Наседкін, І.В. Бабич

*Інститут хімії поверхні ім. О.О. Чуйка Національної академії наук України,  
вул. Олега Мудрака, 17, 03164, Київ, Україна, e-пошта: yuri.plyuto@isc.gov.ua*

*Модельні системи MoO<sub>3</sub>/Al<sub>2</sub>O<sub>3</sub> і MoO<sub>3</sub>/SiO<sub>2</sub> з добре визначеною структурою були цілеспрямовано створені закріпленням MoOCl<sub>4</sub> на поверхні наночастинок пірогенних носіїв Al<sub>2</sub>O<sub>3</sub> і SiO<sub>2</sub>. Подальший гідроліз закріплених груп водною парою та наступна термічна обробка приводили до утворення Mo(VI) оксо-структур на поверхні носіїв. Застосуванням циклів закріплення-гідролізу синтезовано модельні системи MoO<sub>3</sub>/Al<sub>2</sub>O<sub>3</sub> із вмістом молібдену 1.10, 1.92 та 2.34 Мо/нм<sup>2</sup>. Синтезовані системи MoO<sub>3</sub>/SiO<sub>2</sub> мали вміст молібдену 0.82, 1.05 та 1.21 Мо/нм<sup>2</sup>. У синтезованих системах MoO<sub>3</sub>/Al<sub>2</sub>O<sub>3</sub> і MoO<sub>3</sub>/SiO<sub>2</sub> із вмістом молібдену нижче відповідно 2.34 і 1.21 Мо/нм<sup>2</sup> не спостерігалось рентгенівської дифракційної картини, характерної для кристалітів MoO<sub>3</sub>. Це підтверджує, що використаний спосіб синтезу привів до утворення високодисперсних Mo(VI) оксо-*



структур на поверхні як  $Al_2O_3$ , так і  $SiO_2$  носіїв. Ступінь агрегації  $Mo(VI)$  оксо-структур залежить від природи поверхні носія та вмісту молібдену. Збільшення вмісту молібдену на поверхні як  $Al_2O_3$ , так і  $SiO_2$  носіїв приводить до підвищення ступеня агрегації  $Mo(VI)$  оксо-структур. На поверхні  $Al_2O_3$  при вмісті молібдену, що відповідає або перевищує кількість наявних гідроксильних груп, мономерні  $Mo(VI)$  оксо-структури є переважними. При більш високому вмісті молібдену було виявлено утворення полімерних  $Mo(VI)$  оксо-структур. На поверхні  $SiO_2$  при вмісті молібдену, що відповідає або перевищує кількість наявних гідроксильних груп, спостерігалася одночасна присутність мономерних і полімерних  $Mo(VI)$  оксо-структур.

**Ключові слова:** оксид алюмінію, кремнезем, хімія поверхні носіїв, оксид молібдену, поверхневі оксо-структури, УФ-видима спектроскопія.